EWSR1-CREB1 and *EWSR1-ATF1* Fusion Genes in Angiomatoid Fibrous Histiocytoma

Sabrina Rossi,[1] Kàroly Szuhai,[3] Marije Ijszenga,[3] Hans J. Tanke,[3] Lucia Zanatta,[1] Raf Sciot,[4] Christopher D.M. Fletcher,[5] Angelo P. Dei Tos,[1] and Pancras C.W. Hogendoorn[2]

Abstract

Purpose: Angiomatoid fibrous histiocytoma (AFH) is a low-grade mesenchymal neoplasm which usually occurs in children and adolescents. Either *FUS-ATF1* or *EWSR1-ATF1* have been detected in the few cases published, pointing to the interchangeable role of *FUS* and *EWSR1* in this entity. *EWSR1-ATF1* also represents the most frequent genetic alteration in clear cell sarcoma, suggesting the existence of a molecular homology between these two histotypes. We investigated the presence of *EWSR1-CREB1*, recently found in gastrointestinal clear cell sarcoma, and *FUS-CREB1*, as well as the already reported *FUS-ATF1* and *EWSR1-ATF1* in a series of AFH.

Experimental Design: Fourteen cases were analyzed by fluorescence *in situ* hybridization (FISH) on paraffin-embedded tissue sections, using a commercial *EWSR1* probe and custom-designed probes for *FUS, ATF1*, and *CREB1*. In two cases, four-color FISH was also done. Reverse transcription-PCR for the four hypothetical fusion genes was done in one case, for which frozen material was available.

Results: Thirteen cases showed rearrangements of both *EWSR1* and *CREB1*, whereas one case showed the rearrangement of both *EWSR1* and *ATF1*. Four-color FISH confirmed the results in two selected cases. Reverse transcription-PCR showed *EWSR1-CREB1* transcript in the case analyzed.

Conclusion: We identified the presence of either *EWSR1-CREB1* or *EWSR1-ATF1* in all the cases, strengthening the concept of chromosomal promiscuity between AFH and clear cell sarcoma. Either the occurrence of a second unknown tumor-specific molecular event or, perhaps more likely, divergent differentiation programs of the putatively distinct precursor cells of AFH and clear cell sarcoma might be invoked in order to explain the two different phenotypes.

Angiomatoid fibrous histiocytoma (AFH) represents a low-grade mesenchymal neoplasm of uncertain differentiation (1), which usually occurs in the extremities of children and young adults. Morphologically, it is a multinodular proliferation of bland spindle to ovoid eosinophilic cells, sometimes lining pseudoangiomatoid spaces and surrounded by a thick fibrous pseudocapsule, often featuring a prominent lymphoplasmacytic infiltrate. Immunohistochemically, the most relevant finding is represented by the expression of desmin in ~40% of cases, suggesting myogenic differentiation (2, 3). The recurrence rate is between 2% and 11%, and the metastatic rate is <1%. In the context of an uncommon tumor type with a very low rate of metastasis, it is unsurprising that no histologic or immunophenotypic features have thus far been identified to predict patients' outcome.

Until recently, only five cases of AFH studied by cytogenetics (4, 5) and/or molecular genetics (4–7) have been published in detail. Two of them were characterized by the expression of an *FUS-ATF1* fusion gene (4, 6), resulting from a t(12;16)(q13;p11) (ref. 4), whereas in the remaining three cases, a *EWSR1-ATF1* fusion gene was detected (5, 7), resulting from a t(12;22)(q13;q12) (ref. 5). EWSR1 and FUS are members of the TET family, characterized by COOH-terminal RNA-binding domains, which are believed to act as adaptors between transcription and RNA processing (8). The *ATF1* gene encodes a member of the CREB-ATF basic leucine-zipper family of transcription factors, which regulate cell gene expression via homodimeric or heterodimeric DNA-binding to cyclic AMP response elements (9). As a consequence of the fusion of the NH_2 terminus of FUS/EWSR1 with the COOH terminus of ATF1 and the replacement of FUS/EWSR1 RNA-binding domain by ATF1 DNA-binding domain, FUS/EWSR1-ATF1 chimeric proteins might activate transcription independently of cyclic AMP induction.

Interestingly, both *FUS* and *EWSR1* are involved in recombinations as 5′ partners in multiple different tumor types and seem to be functionally interchangeable at least in some of them. In fact, besides the fusion with *ATF* in AFH, both of them rearrange with *ERG* in Ewing's sarcoma (10, 11) and with

Authors' Affiliations: [1]Department of Pathology, Regional Hospital, Treviso, Italy, Departments of [2]Pathology and [3]Molecular Cell Biology, Leiden University Medical Center, Leiden, the Netherlands, [4]Department of Pathology, University Hospital, Catholic University of Leuven, Leuven, Belgium, and [5]Department of Pathology, Brigham and Women's Hospital, Harvard Medical School, Boston, Massachusetts

Received 7/17/07; revised 10/30/07; accepted 11/2/07.

Grant support: European Commission (EUROBONET grant no. 018814).

The costs of publication of this article were defrayed in part by the payment of page charges. This article must therefore be hereby marked *advertisement* in accordance with 18 U.S.C. Section 1734 solely to indicate this fact.

Requests for reprints: Pancras Hogendoorn, Leiden University Medical Center, P.O. Box 9600, L1-Q, 2300 RC Leiden, the Netherlands. Phone: 31-71526-6639; Fax: 31-71524-8158; E-mail: p.c.w.hogendoorn@lumc.nl.

doi:10.1158/1078-0432.CCR-07-1744

Table 1. Clinical data, FISH, and RT-PCR results

Case nos.	Sex/age	Site/depth	Two-color FISH				Four-color FISH	RT-PCR
			EWSR1	*FUS*	*ATF1*	*CREB1*		
1	F/12	Buttock/subcutaneous	R	nnR	nnR	R	—	—
2	M/22	Thigh/subcutaneous	R	nnR	nnR	R	*EWSR1-CREB1*	—
3	F/16	Knee/subcutaneous	R	nnR	nnR	R	—	—
4	M/10	Thigh/subcutaneous	R	nnR	nnR	R	—	—
5	F/30	Arm/subcutaneous	R	nnR	nnR	R	—	—
6	F/10	Arm/subfascial	R	nnR	nnR	R	—	—
7	M/7	Thigh/subcutaneous	R	nnR	nnR	R	—	—
8	F/26	Forearm/subfascial	R	nnR	R	nnR	*EWSR1-ATF1*	—
9	M/4	Forearm/subcutaneous	R	nnR	nnR	R	—	—
10	F/4	Back/subcutaneous	R(pl)	nnR(pl)	nnR(pl)	R(pl)	—	—
11	M/18	Thigh/NA	R	nnR	nnR	R	—	—
12	M/37	Thigh/subcutaneous	R	nnR	nnR	R	—	—
13	M/7	Thigh/prepatellar	R	nnR	nnR	R	—	—
14	M/35	Thigh/subfascial	R	nnR	nnR	R	—	*EWSR1-CREB1*

Abbreviations: R, rearranged; nnR, nonrearranged; (pl), polyploid; NA, not available.

DDIT3 in myxoid liposarcoma (12, 13). Furthermore, four different types of *EWSR1-ATF1* transcript, only three of which were in-frame, including one identical to that reported in AFH (5, 7), have been detected in clear cell sarcoma of soft tissue (14, 15), suggesting the existence of shared genetic mechanisms between AFH and clear cell sarcoma. The recent description of a novel fusion gene, i.e., *EWSR1-CREB1*, in gastrointestinal clear cell sarcoma, raises the possibility that *ATF1* and *CREB1* might also be functionally interchangeable (16).

The genetic parallelism between AFH and clear cell sarcoma, and the functional homology of *EWSR1* and *FUS*, represent a rationale to investigate, in addition to the already reported fusion genes (i.e., *FUS-ATF1* and *EWSR1-ATF1*), the presence of *EWSR1-CREB1* and *FUS-CREB1* in AFH. In fact, recent data presented in abstract form earlier this year (17, 18), and now very recently published in full (19), have shown that *FUS-ATF1* and *EWSR1-ATF1* characterize only a subgroup of AFH and that the most frequent event in AFH indeed seems to be an *EWSR1-CREB1* rearrangement.

In this study, we assessed the prevalence of *FUS/EWSR1-ATF1/CREB1* fusion genes as detected by fluorescence *in situ* hybridization (FISH) in a series of 14 cases of AFH. We also investigated the presence of all four possible fusion transcripts by reverse transcription-PCR (RT-PCR) in one case for which frozen material was available.

Materials and Methods

Patients and tumor samples

Twenty-two cases of AFH with paraffin blocks were retrieved from the consultation files of two of the authors (C.D.M. Fletcher and A.P. Dei Tos) and from the Pathology Department of the Catholic University of Leuven (Leuven, Belgium). Among these, 14 cases, in which adequate tumor tissue for FISH analysis was available, were selected for our study. In addition, frozen tissue was available in one case. Six patients were female and eight were male. Patients' ages ranged from 4 to 37, with a median of 14. Eight tumors were located in the lower extremities, four in the upper extremities and two in the trunk. Clinical information about the depth of the tumors were available in all the cases but one. Four tumors were deep-seated, including three tumors located below the fascia and one tumor located in the prepatellar region, whereas nine tumors were subcutaneous. Patients' clinical data are summarized in Table 1. Morphologically, all lesions showed typical features of AFH, being composed of multinodular proliferation of spindle and ovoid palely eosinophilic cells with a syncytial appearance (Fig. 1A and B). In five cases, prominent pseudovascular spaces filled with RBC were observed (Fig. 1C). In four cases, a peripheral lymphoplasmacytic infiltrate and stromal fibrosis were prominent. Cellular pleomorphism was diffuse in one (Fig. 1D) and focal in three cases.

FISH

Probe selection and labeling. Two-color FISH for *EWSR1*, *FUS*, *ATF1*, and *CREB1* was done on each case. To detect possible rearrangements of *FUS* gene at region 16p11, two bacterial artificial chromosomes (BAC) clones, RP11-196G11, proximal to the breakpoint, and RP11-120K18, distal to the breakpoint, were selected. To investigate *ATF1* at region 12q13.13, BAC clones RP11-189H16 proximal to the breakpoint and RP11-407N8 distal to the breakpoint, were chosen. For *CREB1* at region 2q33.3, we selected two contiguous fosmid clones distal to the breakpoint, G248P81788B12 and G248P89268A6, which were pooled to enhance the signal, and a BAC clone, RP11-167C7 proximal to the breakpoint. All BAC clones were obtained from Wellcome Trust, Sanger Institute. Fosmid clones were obtained from BACPAC Resources. Detailed data about BAC and fosmid clones are summarized in Table 2. DNA from all the BAC and fosmid clones was extracted according to the High pure plasmid isolation kit (Roche Diagnostics GmbH). For *EWSR1*, a commercial split-signal EWSR1 probe (SPoT-Light EWS Translocation Probes; Zymed, Invitrogen), which contains a digoxigenin-labeled proximal part and a biotin-labeled distal part of the *EWSR1* regions, was used.

For the two-color FISH, the probes were labeled either with biotin-11-dUTP or digoxigenin-11-dUTP (Boehringer Mannheim) using a nick translation labeling kit (Boehringer Mannheim and Enzo) according to the manufacturer's instructions. All probes were hybridized on metaphase spreads of lymphocytes to confirm chromosomal location and specificity (data not shown).

For four-color FISH, the CREB1 proximal probe RP11-167C7 and the ATF1 proximal probe RP11-189H16 were labeled by nick translation with Cy5, whereas CREB1 distal probes G248P81788B12 and G248P89268A6 and ATF1 distal probe RP11-407N8 were labeled with Cy3. Four-color FISH for *EWSR1-CREB1* and for *EWSR1-ATF1* was done on two different cases, in which either *EWSR1* and *CREB1* or *EWSR1* and *ATF1*, respectively, were rearranged by two-color FISH (Fig. 3).

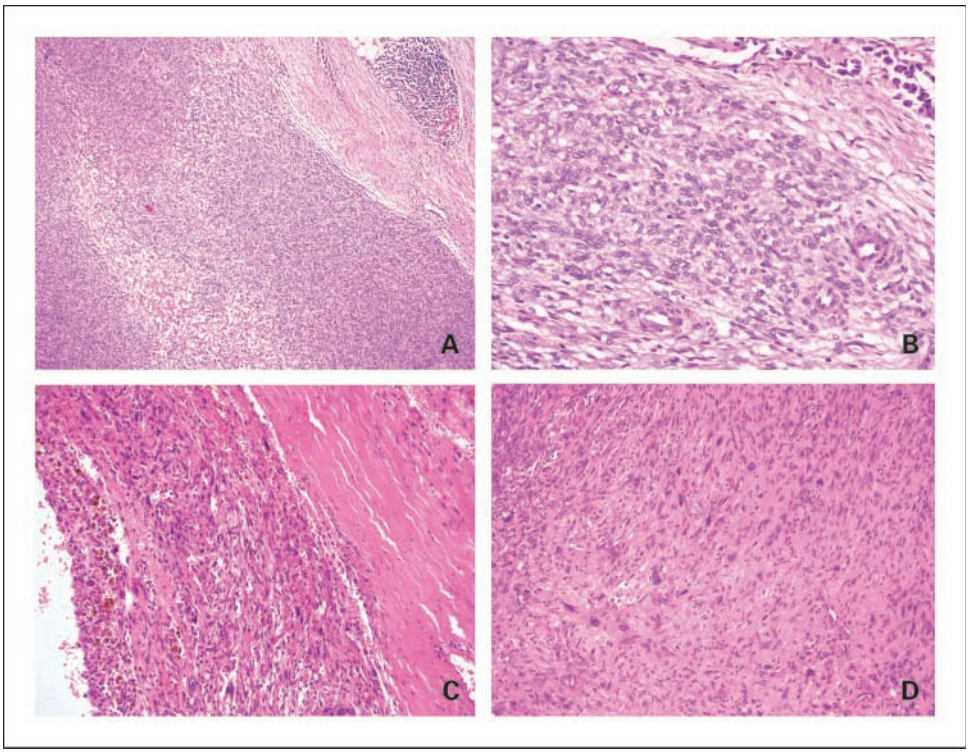

Fig. 1. Morphologic features of AFH. *A,* a case of AFH showing typical pushing borders and peripheral stromal fibrosis with a lymphoid aggregate (case 7; magnification, ×10). *B,* a high-power view of the same case in (*A*), showing the typical spindle and ovoid palely eosinophilic cells (case 7; magnification, ×40). *C,* another case of AFH characterized by the typical pseudovascular spaces with RBCs (case 10; magnification, ×20). *D,* the same case in (*C*) with diffuse nuclear pleomorphism (case 10; magnification, ×20).

Prehybridization, hybridization, and posthybridization treatment of paraffin-embedded tissue sections. Four-micrometer deparaffinized ethanol-dehydrated tissue sections were boiled in 50 mmol/L of Tris-HCl/2 mmol/L EDTA-buffer at pH 9 with a pressure of 1 atm. for 7 min and rinsed with 2× SSC at room temperature. They were subsequently soaked in preheated 1 mol/L of sodium sulfocyanate at 80°C for 45 min, allowed to cool in bidistillated water and rinsed with 2× SSC. They were then incubated with RNase (100 μg/mL) at 37°C, washed twice in 2× SSC, incubated with 4% pepsin/0.02 mol/L HCl at 37°C for 20 min, washed three times with PBS, and ethanol-dehydrated. The labeled DNA probes, except for EWSR1, were diluted in hybridization mixture (60% formamide, 10% dextran sulfate, and 2× SSC; pH 7) to a final concentration of 1 ng/μL. Eleven microliters of hybridization mixture were added onto the slides and probe and target DNA were denatured for 10 min at 80°C. After overnight hybridization at 37°C, two 5-min washes with 2× SSC/0.1% Tween 20 at 37°C, two 5-min washes with 50% formamide/2× SSC at 44°C, one 5-min wash in 2× SSC/0.1 Tween 20 at 44°C, two 5-min washes with 0.1× SSC at 60°C, and one 5-min wash in 1× TBS/0.05% Tween 20 (TNT) at room temperature were done.

For the two-color FISH, all the probes were detected with an indirect method. Sections were incubated with Cy3-labeled streptavidin (1:500; Sigma) and FITC-labeled mouse antidigoxigenin antibody (1:250; Sigma) at 37°C for 30 min. After three 5-min washes with TNT, sections were incubated with FITC-labeled rabbit anti-mouse antibody (1:1,000; Sigma).

For the four-color FISH, because ATF1 and CREB1 probes were directly labeled, only the EWSR1 commercial probe was revealed with an indirect method. Sections were incubated with FITC-labeled mouse antidigoxigenin antibody (1:250; Sigma) and streptavidin LaserPRO 790 (1:250; Molecular Probes, Invitrogen) for 30 min at 37°C. After three 5-min washes with TNT, they were incubated with FITC-labeled rabbit anti-mouse antibody (1:1,000; Sigma) and biotin-labeled goat anti-streptavidin antibody (1:500; Vector Laboratories) with the same conditions. Sections were subsequently washed again three times with TNT and incubated with streptavidin LaserPRO 790 (1:250; Molecular Probes, Invitrogen) for 30 min at 37°C. All the antibodies used were diluted with 0.5% Boehringer blocking reagent/1× TBS (TND). Either for the two-color FISH or for the four-color FISH, after the last antibody incubation, sections were washed thrice with TNT, ethanol-dehydrated, and counterstained with 4′,6-diamidino-2-phenylindole.

Scoring. FISH evaluation was done by counting at least 100 nuclei for each slide. In the samples which showed an abundant reactive lymphoid infiltrate surrounding the tumor, both normal and tumor

Table 2. Data about the BAC and fosmid clones selected

Clone	GenBank ID	Start position*	End position*	Size (kb)	Probe region	Prox-Dist probes gap (kb)	Locus
RP11-196G11	AC135050	30862945	31045174	182.2	FUS (dist)	118.5	16p11.2
RP11-120K18	AC093520	31163677	31329206	165.5	FUS (prox)		16p11.2
RP11-189H16	AC078818	49293862	49433792	139.9	ATF1 (prox)	117	12q13.13
RP11-407N8	AC008121	49550796	49654781	103.9	ATF1 (dist)		12q13.13
RP11-167C7	AC009226	207861196	207999773	138.5	CREB1 (prox)	180	2q33.3
G248P81788B12	AC079767	208191367	208230251	40.8	CREB1 (dist)		2q33.3
G248P89268A6	AC079767	208215933	208254245	38.3	CREB1 (dist)		2q33.3

Abbreviations: Prox, proximal to the breakpoint; dist, distal to the breakpoint.
*According to the Human March 2006 Assembly.

regions were scored. Nuclei with an incomplete set of signals were omitted from the score. Signals were considered colocalized when their distance was equal to or smaller than the size of the hybridization signal. The mean percentage of cells with false split signals for FUS, ATF1, EWSR1, and CREB1 probes, calculated by scoring the nonneoplastic tissue at the peripheral areas, was <1%.

For the two-color FISH, only cases with a complete pattern of two separate red and green signals, and one colocalized or fused signal were considered as rearranged, whereas cases with two colocalized or fused signals were considered as nontranslocated. For the four-color FISH, on nontranslocated cells, the simultaneous hybridization of the four differentially labeled probes was expected to result in a colocalization or fusion of the green and red signals for the normal *EWSR1* gene and of the magenta and blue signals either for the normal *ATF1* or for the normal *CREB1*. In case of either *EWSR1-CREB1* or *EWSR1-ATF1* rearrangement, the green signal of the proximal part of *EWSR1* was expected to colocalize with the blue signal of the distal part of either *CREB1* or *ATF1*, respectively. Additionally, in case of a balanced translocation, the magenta signal of the proximal part of either *CREB1* or *ATF1* was expected to colocalize with the red signal of the distal part of *EWSR1*.

RT-PCR

Frozen tissue was available in one case. RNA was extracted as previously described (20). Two micrograms of total RNA was reverse-transcribed with avian myeloblastosis virus reverse transcriptase (Roche). RT-PCR for *FUS-ATF1*, *FUS-CREB1*, *EWSR1-ATF1*, and *EWSR1-CREB1* was done. RT-PCR for each of the nontranslocated genes was also done. A clear cell sarcoma cell line cDNA was used as a positive control for *EWSR1-ATF1* translocation. All PCR amplifications were done in a 25 μL reaction volume containing 20 mmol/L of Tris-HC1 (pH 8.0), 1.5 mmol/L of $MgC1_2$, 0.2 mmol/L of each deoxynucleotide triphosphate, 2 units of AmpliTaq polymerase (Applied Biosystems), 0.5 μmol/L of each of the forward and reverse primers, and 1 μL of 1:5 diluted, synthesized cDNA. Detailed information about position, length, and direction of the primers used are reported in Table 3. Different primer combinations were used. To detect *FUS-ATF1* rearrangement, the primers 1 (4) and 8 (6) and the primers 2 (4) and 9 (4) were used with an annealing temperature of 60°C and 64°C, respectively. To detect *FUS-CREB1* rearrangement, the primers 1 (4) and 11 (16) and the primers 2 (4) and 12 (16) were used with an annealing temperature of 60°C and 64°C, respectively. To investigate possible *EWSR1-ATF1* and *EWSR1-CREB1* rearrangements, the primers 5 (our) and 8 (6) and the primers 5 (our) and 12 (16) were used with an annealing temperature of 60°C. To detect the normal genes, the primers 1 (4) and 3 (4) for *FUS*, the primers 7 (4) and 9 (4) for *ATF1*, and the primers 10 (our) and 11 (16) for *CREB1* were used with an annealing temperature of 53°C, whereas the primers 7 (4) and 8 (6) for *ATF1*, the primers 1 (4) and 4 (4) for *FUS* and the primers 5 (our) and 6 (our) for *EWSR1* were used with an annealing temperature of 58°C. All PCR reactions consisted of initial denaturation of 4 min, 35 cycles of 30 s at 94°C, 30 s at the annealing temperature chosen for each primer set and 1 min at 72°C, followed by a final extension of 10 min at 72°C. Ten microliters of the PCR products were analyzed by electrophoresis through 1.5% agarose gels stained with ethidium bromide and photographed. For sequence analysis, the amplified cDNA fragment was purified from the gel, using the Qiagen gel extraction kit (Qiagen) and directly sequenced using the dideoxy procedure with an ABI Prism BigDye terminator cycle sequencing ready reaction kit (PE Applied Biosystems) on the Applied Biosystems model 373A DNA sequencing system.

Table 3. Primers used

Primers	Gene	Accession no.	Position	Direction	Reference no.
1	*FUS*	NM_004960	552-575	Forward	4
2	*FUS*	NM_004960	336-358	Forward	4
3	*FUS*	NM_004960	986-1009	Reverse	4
4	*FUS*	NM_004960	1068-1092	Reverse	4
5	*EWSR1*	NM_005243	762-783	Forward	—
6	*EWSR1*	NM_005243	1542-1561	Reverse	—
7	*ATF1*	NM_005171	180-200	Forward	4*
8	*ATF1*	NM_005171	649-627	Reverse	6
9	*ATF1*	NM_005171	918-891	Reverse	4*
10	*CREB1*	BC095407	295-314	Forward	—
11	*CREB1*	BC095407	737-757	Reverse	16
12	*CREB1*	BC095407	791-812	Reverse	16

*Slightly modified from the ones previously reported.

Results

FISH. Two-color FISH for *FUS*, *EWSR1*, *ATF1*, and *CREB1* genes was done on 14 cases. Thirteen cases showed rearrangement of both *EWSR1* and *CREB1* genes, indicating the occurrence of a t(2;22) in these cases (Fig. 2A and B). In nine cases, the number of rearranged cells ranged between 50% and 95%. In four cases, which were morphologically characterized by an abundant inflammatory infiltrate, the number of translocated cells ranged between 10% and 20%. Because these cases showed similar split ratios when analyzed by multiple FISH tests using EWSR1 and CREB1 probes in separate reactions, the presence of a small tumor clone diluted in an abundant reactive background was convincingly proved. Moreover, these cases showed a <1% split signal when analyzed by the ATF1 and FUS FISH.

In one case, which was morphologically characterized by a remarkable degree of pleomorphism (Fig. 1D), besides cells with one colocalized green/red signal, one green signal, and one red signal; cells with two colocalized signals, two red signals, and one green signal; and cells with two colocalized signals, two green signal, and one red signal were also seen, suggesting that this was a polyploid case with an unbalanced translocation. When hybridized with FUS and ATF1 probes, this case showed a proportion of nuclei with multiple colocalized signals, confirming that it was polyploid. One of 14 cases showed the rearrangement of both *EWSR1* and *ATF1* genes in 60% of cells, pointing to the presence of a t(12;22) in this case (Fig. 2C). Notably, none of the cases showed a rearrangement of the *FUS* region.

Four-color FISH was done on two selected cases, in which the signals colocalized, as expected (Fig. 3A and B), confirming *EWSR1-CREB1* rearrangement in one case (Fig. 3C) and *EWSR1-ATF1* rearrangement in another case, which had been already detected by two-color FISH. FISH results are summarized in Table 1.

RT-PCR. RT-PCR for *FUS-ATF1*, *FUS-CREB1*, *EWSR1-ATF1*, and *EWSR1-CREB1* fusion genes was attempted in one case for which frozen material was available. A strong band of 453 bp was obtained (Fig. 4A), by using a forward primer located in exon 6 of *EWSR1* and a reverse primer located in exon 7 of *CREB1* (Fig. 4B). Direct sequencing of the product confirmed the presence of a EWSR1-CREB1 chimeric transcript with a junction between EWSR1 exon 7 and CREB1 exon 7 (Fig. 4C). None of the other three possible chimera (*EWSR1-ATF1*, *FUS-CREB1*, and *FUS-ATF1*) were identified. PCR for *EWSR1-ATF1*

showed a band of the expected size only in the clear cell sarcoma cell line used as control. As control reactions, PCR for the normal genes showed bands of the expected sizes: 457 and 525 bp for *FUS* when primer 1 was used together with primers 3 and 4, respectively, 738 and 469 bp for *ATF1* when primer 7 was used with primers 9 and 8, respectively (Fig. 4A), and 462 bp for *CREB1* and 799 bp for *EWSR1*.

Discussion

Until recently, five cases of AFH with cytogenetic and molecular data have been published in detail. Two of them were characterized by t(12;16) (q13;p11) with *FUS-ATF1* fusion gene (4, 6), whereas the remaining three cases harbored a t(12;22) (q13;q12) with *EWSR1-ATF1* fusion gene (5, 7). Because it was known that AFH and clear cell sarcoma share the *EWSR1-ATF1* fusion gene (5, 7), and because the *EWSR1-CREB1* fusion gene had recently been detected in clear cell sarcoma of the gastrointestinal tract (16), we selected specific probes for *FUS*, *ATF1*, and *CREB1* genes and used them together with a EWSR1 commercial probe to test 14 cases of formalin-fixed paraffin-embedded AFH for *FUS/EWSR1-ATF1/CREB1* rearrangements. In our series, all cases but one showed *EWSR1-CREB1* rearrangement, indicating the presence of a t(2;22)(q34;q12). One of the *EWSR1-CREB1* rearranged cases, which was characterized by a remarkable degree of nuclear pleomorphism, proved to be a polyploid case, which might bear an unbalanced translocation, suggesting, in some cases, the occurrence of more complex karyotypes. However, this molecular feature does not seem to adversely affect the prognosis because the patient has not shown any sign of relapse 7 years after the excision. Furthermore, we confirmed the presence of *EWSR1-CREB1* fusion transcript by RT-PCR in the case for which frozen material was available. The transcript was characterized by the fusion of exon 7 of *EWSR1* and exon 7 of *CREB1*, similarly to the one reported in cases of gastrointestinal clear cell sarcoma (16). Although there were no critical methodologic differences between our study and the previous reports, we could not find any *FUS-ATF1* rearrangement and only one case with *EWSR1-ATF1* rearrangement, suggesting that these are rare molecular events in AFH. Interestingly, the *EWSR1-CREB1* rearrangement was detected in the majority of AFH, therefore confirming and expanding data presented in abstract form earlier this year (17, 18) and now very recently published in full (19). We could not identify any correlation between fusion transcript type and either clinical or pathologic variables, such as patients' age and sex, and the tumors' site, size, or depth in our series. Additionally, no significant clinicopathologic differences were found between the cases in our series and the cases previously published (4–7). However, given the diagnostic difficulty which AFH quite often poses, due to its morphologic variability, our findings do support a new and expanded role for molecular diagnosis in these tumors.

Nonrandom balanced translocations are generally considered tumor-specific and pathogenetically relevant and therefore are used as diagnostic criteria. Two models have been proposed to explain their supposed specificity (21). In the instructive model, the fusion gene resulting from the translocation would instruct the cell to follow a specific program of differentiation through gene expression changes, with consequent development of a specific tumor phenotype. Alternatively, in the context-dependent model, the specificity would be determined by a selection process for which only one or a limited number of cell lineages, with a particular chromatin status in specific regions and/or with certain survival pathways, would allow the occurrence of a specific translocation and/or would tolerate its biological consequences. However, an increasing number of examples of chromosomal promiscuity have been detected in recent years, for example, the *ETV6-NTRK3* fusion gene, which is found in infantile fibrosarcoma, mesoblastic nephroma,

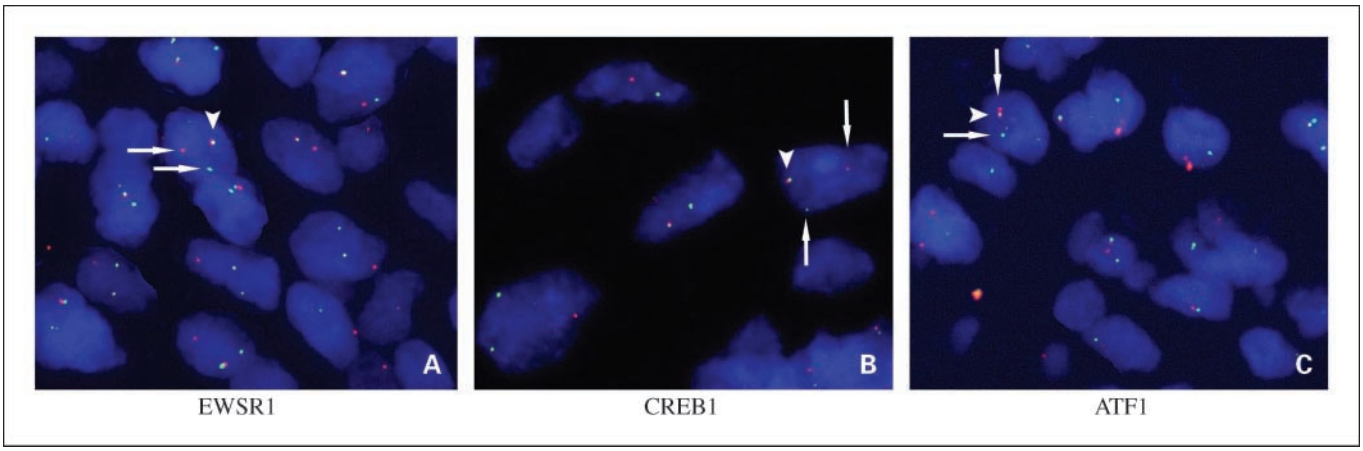

Fig. 2. Overview of interphase FISH results on formalin-fixed paraffin-embedded tissue. *A,* a case showing *EWSR1* rearrangement by interphase FISH using *EWSR1* break-apart probe (Zymed). Proximal and distal *EWSR1* regions are hybridized by separate probes (*green* and *red*, respectively). The presence of separate green and red signals indicates a rearrangement of the *EWSR1* region on chromosome 22 (*arrows*), whereas colocalized signals represent the normal *EWSR1* region on chromosome 22 (*arrowhead*). *B,* the same case as in (*A*) with *CREB1* rearrangement. The distal *CREB1* region is hybridized to two contiguous fosmid probes, G248P81788B12 and G248P89268A6, labeled with biotin-11-dUTP and revealed by Cy3-labeled streptavidin (*red*), whereas the proximal *CREB1* region is hybridized to the BAC probe RP11-167C7, labeled with digoxigenin-11-dUTP, and revealed by FITC-labeled mouse antidigoxigenin antibody (*green*). Although separate green and red signals indicate the rearrangement of *CREB1* region on chromosome 2 (*arrows*), colocalized signals represent the normal *CREB1* region on chromosome 2 (*arrowhead*). *C,* only one case showed *ATF1* rearrangement. The proximal *ATF1* region is hybridized to the BAC probe RP11-189H16, labeled with digoxigenin-11-dUTP, and revealed by FITC-labeled mouse antidigoxigenin antibody (*green*), whereas the distal *ATF1* region is hybridized to the BAC probe RP11-407N8, labeled with biotin-11-dUTP, and revealed by Cy3-labeled streptavidin (*red*). Rearrangement of the *ATF1* region on chromosome 12 is indicated by the presence of separate red and green signals (*arrows*), whereas colocalized signals represent normal *ATF1* region on chromosome 12 (*arrowhead*).

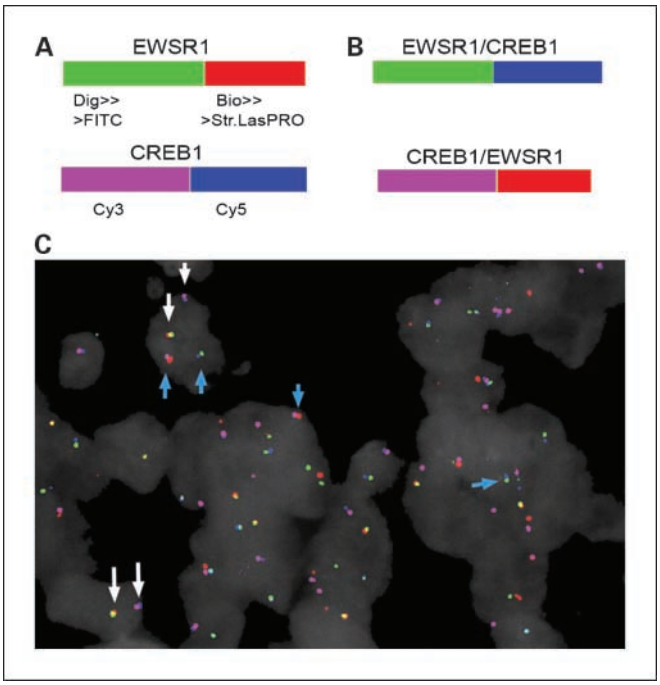

Fig. 3. *A,* four-color FISH labeling scheme. EWSR1 commercial probe (Zymed) contains a digoxigenin-labeled proximal part and a biotin-labeled distal part and was revealed by a three-step indirect method, which resulted in a EWSR1 probe showing a FITC-labeled proximal part (*green*) and a LaserPro-labeled distal part (*red*). CREB1 proximal probe was directly labeled with Cy5 (*magenta*), whereas CREB1 distal probes were directly labeled with Cy3 (*blue*). *B,* schematic representation of *EWSR1-CREB1* rearrangement detected by four-color FISH. Colocalization or fusion of the green signal of the proximal part of *EWSR1* with the blue signal of the distal part of *CREB1* was expected in the case of *EWSR1-CREB1* rearrangement. Due to the balanced nature of the rearrangement, a fusion between the proximal *CREB1* (*magenta*) and distal *EWSR1* (*red*) should be present. *C,* EWSR1-CREB1 rearrangement detected by four-color FISH. The magenta and blue colocalized signals indicate the normal *CREB1* region on chromosome 2, whereas the red and green signals indicate *EWSR1* normal region on chromosome 22 (*white arrowheads*). The green and blue colocalized signals indicate the rearrangement involving proximal *EWSR1* region on chromosome 22 and distal *CREB1* region on chromosome 2. The colocalization of magenta and red indicates the *CREB1-EWSR1* reciprocal fusion gene (*blue arrows*).

acute myeloid leukemia, and secretory breast carcinoma or the *ASPSCR1-TFE3* fusion gene, which represents a shared genetic aberration of both alveolar soft part sarcoma and pediatric forms of renal cell carcinoma (22, 23). Previous findings in AFH (5, 7, 18, 19), and our findings, highlight an additional example of chromosomal promiscuity, demonstrating that AFH and clear cell sarcoma, which are two morphologically, immunophenotypically, and clinically different tumor entities, share the same fusion genes, specifically *EWSR1-CREB1* and *EWSR1-ATF1*. The occurrence of other unknown downstream genetic events might explain the two distinct phenotypes. Interestingly, twin studies in childhood leukemia have well documented that tumor-specific chromosomal translocations are not always able to induce overt disease and that a second hit might be required. For instance, acute lymphoblastic leukemia is initiated by the *ETV6-RUNX1* fusion gene, but only the subsequent deletion of 12p, with consequent loss of the nonrearranged *ETV6* gene, leads to final clinically evident leukemia development (24). This intriguing model does not seem to be applicable to clear cell sarcoma. In fact, given that *EWSR1-ATF1* knockdown has a growth-suppressive effect on soft agar colonies of clear cell sarcoma cell lines (25), it is likely that the translocation per se is sufficient for cell transformation in clear cell sarcoma. Although theoretically, the occurrence of additional molecular events could still be invoked to explain the alternative phenotype of AFH, this possibility seems remote. It is more reasonable to hypothesize that the two distinct phenotypes of AFH and clear cell sarcoma might be the result of differentiation programs already present in two different tumor progenitor cells. Among the possible candidate genes involved, *M-MITF* and *SOX10* might be considered. In fact, there is evidence that the *M-MITF* promoter is transactivated by the *EWSR1-ATF1* fusion gene in the presence of SOX10 in clear cell sarcoma cell lines, leading to melanocytic differentiation, tumor cell survival, and proliferation (25), and that both *M-MITF* and *SOX10* are highly expressed in clear cell sarcoma (15, 26). Given that *M-MITF* and *SOX10* were not detected in three cases of AFH tested, which were characterized by an EWSR1-ATF1 fusion gene (5, 7), it is reasonable to think that the *EWSR1-ATF1* fusion gene in AFH targets other genes rather than *M-MITF*. A possible explanation might be found in the putative myoid nature of the AFH precursor cell, which would lack expression of *SOX10*, which is typically restricted to neural crest–derived cells. However, the scenario becomes more complex when clear cell sarcoma in gastrointestinal locations is considered. In fact, despite the presence of either *EWSR1-ATF1* or *EWSR1-CREB1*, gastrointestinal clear cell sarcomas do not express *M-MITF* and lacks specific melanocytic markers in the majority of the cases (16). Furthermore, SOX10 levels in

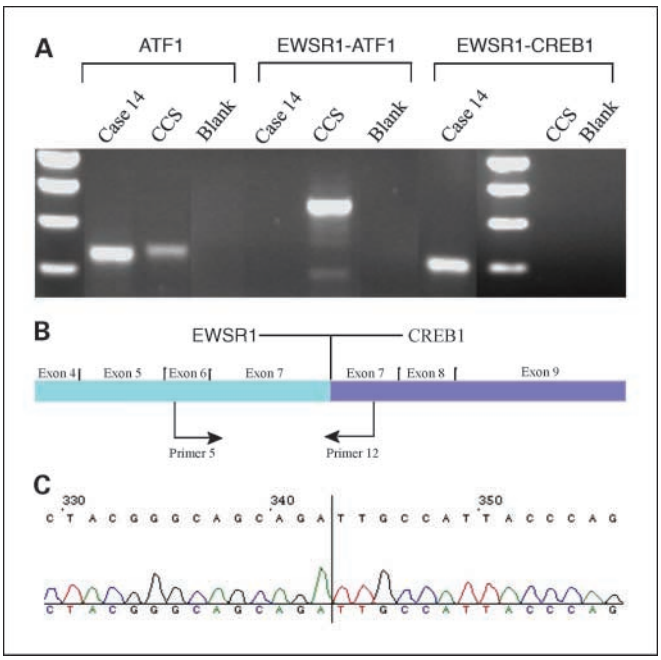

Fig. 4. *A,* RT-PCR results. RT-PCR was done in one case (case 14) for which frozen tissue was available. Detection of strong bands of the expected size (469 bp) obtained with the use of specific primers for *ATF1* normal gene, primers 7 and 8, confirmed the good quality of the cDNA extracted. RT-PCR with specific primers for *EWSR1-ATF1* fusion gene, primers 5 and 8, showed a band of the expected size only in the clear cell sarcoma cell line cDNA, used as positive control. RT-PCR with specific primers for *EWSR1-CREB1* fusion gene, primers 5 and 12, showed a strong band of 453 bp in case 14. *B,* schematic representation of EWSR1-CREB1 chimeric transcript. EWSR1-CREB1 chimeric transcript consisted of a junction between *EWSR1* exon 7 and *CREB1* exon 7. Primer 5 was located in exon 6 of *EWSR1* and primer 12 was located in exon 7 of *CREB1*. *C,* direct sequencing of the RT-PCR product. The *EWSR1-CREB1* fusion involved codon 265 of *EWSR1* (NM.005243) and codon 169 of CREB1 (BC095407).

one case of gastrointestinal clear cell sarcoma were not significantly different from the levels in non–gastrointestinal clear cell sarcoma by gene expression profiling, suggesting that gastrointestinal and non–gastrointestinal clear cell sarcoma have a common *SOX10*-expressing neuroectodermal precursor, which in a gastrointestinal location, might have lost the potential to differentiate along the melanocytic lineage (16). *In vitro* studies with transfection of the *EWSR1-ATF1/CREB1* fusion gene into different cell lineages could potentially help to clarify the pathogenetic mechanism.

In this study, we assessed the prevalence of *FUS/EWSR1-ATF1/CREB1* fusion genes by interphase FISH in a series of 14 cases of AFH. We concluded that the large majority of AFH are characterized by rearrangement of *EWSR1* with one member of the CREB/ATF family of transcription factors, the *EWSR1-CREB1* fusion gene being the most frequent molecular abnormality. These data point to the potential diagnostic role of molecular testing in a clinical setting. Furthermore, we verified that the EWSR1-CREB1 transcript is identical to the one which characterizes gastrointestinal clear cell sarcoma, strengthening the molecular homology between AFH and clear cell sarcoma.

Acknowledgments

We thank Drs. Roberta Maestro and Daniela Gasparotto from CRO of Aviano, Drs. Salvatore Romeo and Anne Marie Cleton-Jansen from LUMC of Leiden for critical discussion, and Marja van der Burg for technical assistance in performing FISH experiments.

References

1. Fanburg-Smith JC, Dal Cin P. Angiomatoid fibrous histiocytoma. Fletcher CDM, Unni KK, Mertens F. WHO classification of tumours. Pathology and genetics of tumours of soft tissue and bone. 194–5. IARC Press. Lyon, 2002.
2. Fletcher CD. Angiomatoid "malignant fibrous histiocytoma": an immunohistochemical study indicative of myoid differentiation. Hum Pathol 1991;22:563–68.
3. Fanburg-Smith JC, Miettinen M. Angiomatoid "malignant" fibrous histiocytoma: a clinicopathologic study of 158 cases and further exploration of the myoid phenotype. Hum Pathol 1999;30:1336–43.
4. Waters BL, Panagopoulos I, and Allen EF. Genetic characterization of angiomatoid fibrous histiocytoma identifies fusion of the FUS and ATF-1 genes induced by a chromosomal translocation involving bands 12q13 and 16p11. Cancer Genet Cytogenet 2000;121:109–16.
5. Hallor KH, Mertens F, Jin Y, Meis-Kindblom JM, Kindblom LG, Behrendtz M, et al. Fusion of the EWSR1 and ATF1 genes without expression of the MITF-M transcript in angiomatoid fibrous histiocytoma. Genes Chromosomes Cancer 2005;44:97–102.
6. Raddaoui E, Donner LR, Panagopoulos I. Fusion of the FUS and ATF1 genes in a large, deep-seated angiomatoid fibrous histiocytoma. Diagn Mol Pathol 2002;11:157–62.
7. Hallor KH, Micci F, Meis-Kindblom JM, et al. Fusion genes in angiomatoid fibrous histiocytoma. Cancer Lett 2007;25:158–63.
8. Law WJ, Cann KL, Hicks GG. TLS, EWS, and TAF15: a model for transcriptional integration of gene expression. Brief Funct Genomic Proteomic 2006;5:8–14.
9. Persengiev SP, Green MR. The role of ATF/CREB family members in cell growth, survival and apoptosis. Apoptosis 2003;8:225–8.
10. Shing DC, McMullan DJ, Roberts P, et al. FUS/ERG gene fusions in Ewing's tumors. Cancer Res 2003;63:4568–76.
11. Kaneko Y, Kobayashi H, Handa M, Satake N, Maseki N. EWS-ERG fusion transcript produced by chromosomal insertion in a Ewing sarcoma. Genes Chromosomes Cancer 1997;18:228–31.
12. Crozat A, Aman P, Mandahl N, Ron D. Fusion of CHOP to a novel RNA-binding protein in human myxoid liposarcoma. Nature 1993;363:640–4.
13. Panagopoulos I, Höglund M, Mertens F, Mandahl N, Mitelman F, Aman P. Fusion of the EWS and CHOP genes in myxoid liposarcoma. Oncogene 1996;12:489–94.
14. Panagopoulos I, Mertens F, Debiec-Rychter M, et al. Molecular genetic characterization of the EWS/ATF1 fusion gene in clear cell sarcoma of tendons and aponeuroses. Int J Cancer 2002;99:560–7.
15. Antonescu CR, Tschernyavsky SJ, Woodruff JM, Jungbluth AA, Brennan MF, Ladanyi M. Molecular diagnosis of clear cell sarcoma: detection of EWS-ATF1 and MITF-M transcripts and histopathological and ultrastructural analysis of 12 cases. J Mol Diagn 2002;4:44–52.
16. Antonescu CR, Nafa K, Segal NH, Dal Cin P, Ladanyi M. EWS-CREB1: a recurrent variant fusion in clear cell sarcoma-association with gastrointestinal location and absence of melanocytic differentiation. Clin Cancer Res 2006;12:5356–62.
17. Terra SBSP, Folpe AL, Weiss SW, et al. Frequency and characterization of ATF1—fusion genes in angiomatoid fibrous histiocytoma [abstract 76]. Mod Pathol 2007;20.
18. Antonescu CR, Dal Cin P, Nafa K, Teot LA, Fletcher CDM, Ladanyi M. EWS-CREB1 is the predominant gene fusion in so-called angiomatoid fibrous histiocytoma [abstract 31]. Mod Pathol 2007;20.
19. Antonescu CR, Dal Cin P, Nafa K, et al. EWSR1-1 is the predominant gene fusion in angiomatoid fibrous histiocytoma. Genes Chromosomes Cancer 2007;46:1051–60.
20. Baelde HJ, Cleton-Jansen AM, van Beerendonk H, Namba M, Bovee JV, Hogendoorn PC. High quality RNA isolation from tumours with low cellularity and high extracellular matrix component for cDNA microarrays: application to chondrosarcoma. J Clin Pathol 2001;54:778–82.
21. Helman LJ, Meltzer P. Mechanisms of sarcoma development. Nat Rev Cancer 2003;3:685–94.
22. Stenman G. Fusion oncogenes and tumor type specificity—insights from salivary gland tumors. Semin Cancer Biol 2005;15:224–35.
23. Lannon CL, Sorensen PH. ETV6-3: a chimeric protein tyrosine kinase with transformation activity in multiple cell lineages. Semin Cancer Biol 2005;15:215–23.
24. Greaves MF, Maia AT, Wiemels JL, Ford AM. Leukemia in twins: lessons in natural history. Blood 2003;102:2321–33.
25. Davis IJ, Kim JJ, Ozsolak F, et al. Oncogenic MITF dysregulation in clear cell sarcoma: defining the MiT family of human cancers. Cancer Cell 2006;9:473–84.
26. Li KK, Goodall J, Goding CR, et al. The melanocyte inducing factor MITF is stably expressed in cell lines from human clear cell sarcoma. Br J Cancer 2003;89:1072–8.

Clinical Cancer Research

EWSR1-CREB1 and *EWSR1-ATF1* Fusion Genes in Angiomatoid Fibrous Histiocytoma

Sabrina Rossi, Kàroly Szuhai, Marije Ijszenga, et al.

Clin Cancer Res 2007;13:7322-7328.